Polymerization of Epoxidized Vegetable Oil Derivatives: Ionic-Coordinative Polymerization of Methylepoxyoleate

E. DEL RIO, M. GALIÀ, V. CÁDIZ, G. LLIGADAS, J. C. RONDA

Departament de Química Analítica i Química Orgánica, Universitat Rovira i Virgili, Campus Sescelades,

Marcel.lı´ Domingo s/n., 43007 Tarragona, Spain

ABSTRACT: Ring-opening polymerization of epoxidized methyloleate (EMO) with various ionic-coordinative initiators have been studied and compared with other internal epoxy monomers: benzyl 9,10-epoxyoleoylether and cis-4,5-epoxyoctane. The structure and molecular weight of the resulting polymers have been studied by ^{1}H- and ^{13}C-NMR, MALDI-TOF-MS, and size exclusion chromatography analysis. Polymers with higher molecular weight than those obtained with conventional cationic catalyst are obtained. These materials have been found to consist of a complex mixture of cyclic and linear polymer chains with different chain ends that can be related to the catalyst nature and the occurrence of two main polymerization mechanisms, the cationic and the ionic-coordinative. In the polymerization of EMO, transesterification by-side reactions leading to ester linkages in the main chain have been identified. These undesired reactions have been suppressed by copolymerization with small amounts of tetrahydrofuran with no substantial decrease in the polymer yield and molecular weight. Finally, the polymerization of EMO has been tested in a larger scale to prepare a renewable resource-based polyether as starting material to produce polyether polyols for polyurethane applications.

KEYWORDS: MALDI; microstructure; polyethers; renewable resources; ring-opening polymerization

INTRODUCTION

Sustainable development has become the key ideal of the 21st Century. In the search for sustainable chemistry, considerable importance is being attached to renewable raw materials, which exploit the synthetic capabilities of nature and may eventually substitute fossil and depleting feedstocks.[1] Oils and fats of vegetable and animal origin make up the greatest proportion of the current consumption of renewable raw materials in the chemical industry because of their availability, structural variety, and chemical versatility. Vegetable oils containing unsaturated fatty acids can be used in polymerizations to make biobased polymers.[2–5] Moreover, numerous fatty acids are now available in a purity that makes them attractive for synthesis and as raw materials for the chemical industry.[6] Although they possess double bonds, which are used as reactive sites in coatings, they cannot be converted easily to high-molecular-weight products without the introduction of more reactive functional groups, such as hydroxyl, epoxy, or carboxyl groups. Epoxidation is one of the most important functionalization reactions of the C=C double bond. The chemistry of the Prileshajev epoxidation of unsaturated fatty compounds is well known,[7,8] but many other epoxidation methods have been described.[9–13] Epoxidized fatty acids are suitable monomers for ring-opening polymerizations.[14] The preparation of polyols from fatty acids and oils for general polyurethane use has been the subject of many studies;[15–17] however, limited attention has been paid to the preparation of polyether polyols. Polyether polyols with molecular weights of 200–10,000 g/mol[18] are important building blocks for polyurethane applications. Polyether polyols are usually produced by the anionic ringopening polymerization of alkylene oxides, such as ethylene oxide or propylene oxide. In contrast, polyether polyols from longer chain or functionalized epoxides are rare because of their lower reactivity due to a higher sterical hindrance, interaction with the catalyst sites, and the occurrence of side reactions. The cationic ring-opening polymerization of higher epoxides usually leads to low-molecular-weight polyethers because of the occurrence of backbiting processes but has been applied in the case of terminal epoxidized fatty compounds.[19–21] The polymerization of internal epoxidized fatty acid derivatives such as methyl epoxy oleate (EMO) is expected to proceed in a more difficult way because of the higher steric demand of the epoxy groups. However, the resulting comb-like polyethers having side chain ester groups can be used to produce fully renewable polyethers with varying amounts of primary hydroxyl groups by controlled reduction of the ester groups. We have already used this methodology to synthesize low-molecular-weight polyols from EMO that were used to prepare rigid polyurethanes.[22] The cationic polymerization of EMO led to polyethers with maximum molecular weight of 1200 Da; hence, achieving highmolecular-weight renewable polyether polyols suitable for the preparation of flexible polyurethanes is still a challenge that excludes the use of either cationic or anionic catalysts.

Coordinative ring-opening polymerization of epoxides has been intensively studied since the late 1950s, and various coordinative catalysts mainly based on aluminum and zinc alkyls have been developed.[23–25] Some of these initiating systems also allow the polymerization of epoxides having additional functional groups in the molecule. Polymers from phenylglycidylethers, which contain methyl ester groups of different chain lengths in the para position, were synthesized by Ronda et al.[26] Shih and Tirell[27] studied the polymerization of 4,5-epoxypentanol esters, whereas Vogl and coworkers[28–30] described the polymerization of x-epoxy alkanoates using the so-called ‘‘Vandenberg’’ catalyst.

Hydrolysis or solvolysis of organoaluminum compounds generally leads to complex product mixtures, which are highly dependent on the reaction conditions. To avoid uncertainty concerning the catalyst preparation, similar catalyst systems based on commercially available aluminoxanes have also been described.[31] In this way, catalyst systems based on methyl aluminoxane (MAO) and tetraisobutylaluminoxane (TIBAO) have been used to polymerize ω-C10, C11, and C14 epoxy carboxylic acid methyl esters, 1,2-decene oxide, silylated 10,11-epoxyundecanol, 9-decenoic, and 13-tetradecenoic methyl esters monomers.[32]

Until now, the ionic-coordinative ring-opening polymerization of internal epoxidized fatty acid epoxies has not received much attention; thus, in this article, we report the synthesis and characterization of polyethers from methyl 9,10-epoxyoctadecenoate (epoxidized methyl oleate, EMO), as precursor for high-molecular-weight renewable polyether polyols. The polymerization of benzyl 9,10-epoxyoctadecenylether (BEO) and 4,5-epoxyoctane (EO) as model monomers has been also considered (Scheme 1).

EXPERIMENTAL

Materials

Benzyl chloride 99%, tetrabutylammonium hydrogen sulfate, and triflouroacetic anhydride were purchased from Fluka. Methyl oleate 99%, oleyl alcohol (85%), 3-chloroperbenzoic acid (MCPBA), H_2O_2 30%, triethylaluminum 25 wt % (1.9M) solution in toluene, TIBAO, 10 wt % solution in toluene, and triisobutylaluminum 25 wt % (1.0M) solution in toluene were purchased from Aldrich and used as received. Methyl oleate 90plus® was kindly supplied by T+T Oleochemie, and cis-4-octene 97% was purchased from Alfa Aesar. Anhydrous sulfur-free toluene, diethyl ether, and tetrahydrofuran (THF) were prepared by refluxing with sodium/benzophenone.

Synthesis of Benzyl-9-octadecenylether

In a 500-mL round bottom flask, 97 g (0.36 mol) of oleyl alcohol, 57 g (0.45 mol) of benzyl chloride, toluene (100 mL), 6.1 g (0.018 mol, 5 mol %) of tetrabutylammonium hydrogen sulfate, and 40 mL (0.5 mol) of 50% (w/w) aqueous solution of NaOH were introduced. The mixture was stirred vigorously at room temperature. The reaction was followed by TLC until completion (24 h). The organic layer was decanted and washed several times with water, 5% HCl, 5% $NaHCO_3$, and brine, dried over anhydrous $MgSO_4$, and concentrated under reduced pressure to give a yellow liquid that was fractionated under vacuum. The fraction between 160 and 162 °C (0.1 mmHg) was collected as colorless oil (92 g, yield 71%).

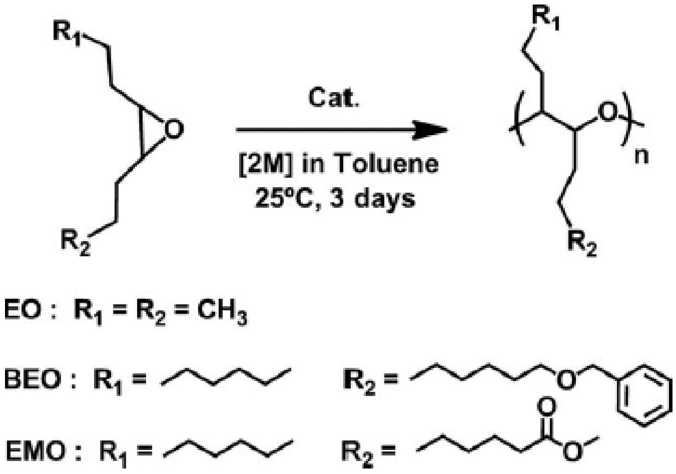

SCHEME 1 Chemical structures of monomers and polyethers.

^{1}H-NMR ($CDCl_3$, tetramethylsilane [TMS], δ in ppm): 7.45–7.35 (2 H, m, o-ArH), 7.35–7.25 (3 H, m, m,p-ArH), 5.50–5.35 (2 H, m, -CH=CH-), 4.55 (2 H, s, $-OCH_2Ar$), 3.52 (2 H, t, J = 6.6 Hz, $-CH_2$-O-Bn), 2.2–2.0 (4 H, m, $-CH_2$-CH=), 1.8– 1.6 (2 H, m, $-CH_2-CH_2$-O-), 1.6–1.2 (m, aliphatic backbone), 0.95 (3 H, $-CH_3$).

^{13}C-NMR ($CDCl_3$, TMS, δ in ppm): 138.9 (-CH_2-CAr), 130.2 and 130.1 (-C=C-), 128.6 (m-Ar), 127.9 (o-Ar), 127.7 (p-Ar), 73.1 (-O-CH_2-Ar), 70.8 (-CH_2-O-CH_2Ar), 32.9 (-CH_2CH=CH-), 32.2 (-CH_2-CH_2-CH3), 31-29 (aliphatic backbone), 27.5 (-CH_2CH_2CH=CH-), 26.5 (-CH_2-CH_2-O-CH_2Ar), 23.0 (-CH_2-CH_3), 14.4 (-CH_3).

Synthesis of EO, BEO, and EMO

Methyl oleate 99% (25 g, 0.084 mol), methyl oleate 90% (89 g, 0.30 mol), and benzyloleylether (36 g, 0.10 mol) were epoxidized with H_2O_2 (16%) using a quaternary ammoniumtetrakis(diperoxotunstato)phosphate catalyst[9,33] and following a procedure described by Venturello and D'Aloisio.[34] EMO and BEO were purified by crystallization in 10 mL/g of acetone at -18 ºC twice, filtration over a short path of silica gel using hexane/ethyl acetate 8/1 as eluent, concentrated, and finally dried under vacuum for 48 h at 40 ºC to yield transparent colorless oils.

EMO from 99% methyl oleate 20.6 g (78%) purity 98% (GC). EMO from 90% methyl oleate 67.5 g (72%) purity 94% (GC). BEO 26.6 g (71%) purity 96% (GC).

4-cis-Octene (20 g, 0.178 mol) was epoxidized with dry MCPBA in DCE following a reported procedure.[35] 4-Epoxyoctene was distilled over calcium hydride at reduced pressure collecting the fraction boiling at 47–48 ºC (2 mmHg) (literature 95 C/60 mbar[36]), which was stored under argon. Yield 18.7 g (82%) purity 98% (GC).

BEO

^{1}H-NMR ($CDCl_3$, TMS, δ in ppm): 7.45–7.35 (2 H, m, o-ArH), 7.35–7.25 (3 H, m, m,p-ArH), 4.51 (2 H, s, -OCH_2Ar), 3.47 (2 H, t, J = 6.6 Hz, -CH_2-O-Bn), 2.91 (2 H, m, epoxide), 1.7–1.5 (2 H, m, -CH_2-CH_2-O-), 1.5-1.2 (m, aliphatic backbone), 0.90 (3 H, t, -CH_3).

^{13}C-NMR ($CDCl_3$, TMS, δ in ppm): 138.3 (-CH_2-CAr), 128.5 (m-Ar), 127.7 (o-Ar), 127.6 (p-Ar), 73.0 (-O-CH_2-Ar), 70.6 (-CH_2-O-CH_2Ar), 57.4 (-CHO), 32.0 (-CH_2-CH_2-CH_3), 30.5–28.5 (aliphatic backbone), 28.0 (-CH_2-CHO), 26.8 (-CH_2-CH_2-CHO), 26.3 (-CH_2-CH_2-O-CH_2Ar), 22.8 (-CH_2-CH_3), 14.3 (-CH_3).

Catalysts

TIBAO 25 wt % in toluene catalyst was used as received. TIBAO/triisobutylaluminum (1:1) system (TIBAO/$^{i}Bu_3Al$) was prepared ''in situ'' by adding the necessary amount of triisobutylaluminum (solution 1.0 M in toluene), after the addition of TIBAO.

The Vandenberg catalyst $(C_2H_5)_3Al/H_2O$ (mole ratio 1:0.5) was prepared as follows. To a dry Schlenck, equipped with a teflon-coated stirring bar and a rubber seal septum, 60 mL of 25% solution of TEA in toluene (50.9 g, 111 mmol) and 30 mL of anhydrous ethyl ether were carefully transferred in this order with an argon-purged double-ended needle. The Schlenck was cooled in an ice-water bath, and then distilled water (1.0 mL, 55.5 mmol) was added dropwise to the stirred solution using a microsyringe, over a 1 h period. A slight positive pressure of nitrogen was maintained throughout the apparatus to sweep away the ethane formed during the reaction. After the addition was completed, the colorless solution was stirred for 6 h to allow completion of the reaction. The aluminum concentration (1.25M) in the resulting colorless solution was determined gravimetrically using 8hydroxyquinoline.[37] The catalyst solution was stored in a refrigerator and aged for 1 week before it was used.

Polymerizations

Before its polymerization, EMO and BEO were dried by stirring overnight over freshly activated 4 Å molecular sieves and filtered under argon atmosphere. All operations were performed under dry argon using standard Schlenck techniques.

Small-Scale Polymerizations

In a typical polymerization, in a 25-mL Schlenck tube, 5 mmol of monomer and the necessary amount of anhydrous toluene to obtain a 2M solution were introduced using a syringe. After cooling to 0 ºC, the necessary amount of catalyst solution to obtain a 10/1 monomer-aluminum ratio was added using a microsyringe. The mixtures were homogenized, allowed to reach room temperature, and maintained at 25 ºC in a controlled bath for 72 h. The polymerization was stopped by adding 20 mL of 5 wt % HCl in MeOH solution and stirred for 12 h. After sedimentation, the supernatant was decanted; the polymer was dissolved in THF, and precipitated once in 5% HCl in MeOH and twice in pure MeOH (50 mL/g). The resulting white rubber-like polymer was dried under vacuum for 24 h at 40 ºC.

Polymerizations with Vandenberg catalyst in the presence of THF were carried out following the same procedure but adding 0.02 mL (0.25 mmol) of anhydrous THF to the monomer solution before the addition of the catalyst. The polymer conversion and molecular weight of the obtained polymers are given in Table 1.

PEO

^{1}H-NMR ($CDCl_3$, TMS, δ in ppm): 3.4–3.2 (polyether backbone), 1.7–1.2 (aliphatic backbone), 1.0–0.85 (m, -CH_3).

^{13}C-NMR ($CDCl_3$, TMS, δ in ppm): 81–79 (polyether backbone), 33–31 (-CH_2-CHO-), 21–19 (-CH_2-CH_3), 14.7 (-CH_3).

PBEO

^{1}H-NMR ($CDCl_3$, TMS, δ in ppm): 7.4–7.2 (aromatic backbone), 4.48 (2 H, m, -O-CH_2-Ar), 3.44 (-CH_2-O-Bn), 3.4–3.2 (polyether backbone), 1.7–1.5 (2 H, m, -CH_2-CH_2-O-), 1.5–1.2 (m, aliphatic backbone), 0.89 (m, -CH_3).

^{13}C-NMR ($CDCl_3$, TMS, δ in ppm): 138.9 (-CH_2-CAr), 128.5 (m-Ar), 127.7 (o-Ar), 127.6 (p-Ar), 82-79 (polyether backbone), 73.0 (-O-CH_2-Ar), 70.7 (-CH_2-O-CH_2Ar), 32.2 (-CH_2-CH_2-CH_3), 31.5–29.0 (aliphatic backbone), 28.0– 26.5 (-CH_2-CHO and -CH_2-CH_2-CHO), 26.6 (-CH_2-CH_2-O-CH_2Ar), 22.9 (-CH_2-CH_3), 14.4 (-CH_3).

PMEO

^{1}H-NMR ($CDCl_3$, TMS, δ in ppm): 3.63 (s, -O-CH_3), 3.40– 3.10 (m, polyether backbone), 2.27 (t, -CH_2-CO_2-), 1.70– 1.10 (m, -CH_2-aliphatic backbone), 0.85 (t, -CH_3).

^{13}C-NMR ($CDCl_3$, TMS, δ in ppm): 173.8 (-CO_2Me), 82–78 (polyether backbone), 51.5 (-OMe), 34.2 (-CH_2-CO_2Me), 32.2 (-CH_2-CH_2-CH_3), 31.5–29.0 (aliphatic backbone), 28.0–26.0 (-CH_2-CHO and -CH_2-CH_2-CHO), 25.2 (-CH_2-CH_2-CO_2Me), 22.9 (-CH_2-CH_3), 14.3 (-CH_3).

Large-Scale Polymerization of EMO

In a dry 250-mL flask under argon atmosphere, 31.2 g (0.1 mol) of the EMO obtained from 90% methyl oleate, 40 mL of toluene, and 0.4 mL (5 mmol) of THF were introduced. After cooling to 0 ºC, 8.0 mL of catalyst solution were added. The mixture was homogenized, allowed to reach room temperature, and maintained at 25 ºC in a controlled bath for 72 h. The polymerization was stopped by adding 150 mL of 5 wt % HCl in MeOH solution and stirred vigorously for 12 h. The supernatant was decanted, and the polymer was dissolved in 100 mL of THF and precipitated once in 1.5 L of 5% HCl in MeOH and twice in 1.5 L of pure MeOH. The resulting polymer was dried in vacuum during 48 h at 40 ºC giving 15.7 g (50%) of a white solid.

Reduction Tests

In a 250-mL round bottom flask under argon atmosphere, 1.88 g (6.0 mmol) of PEMO (obtained with Vandenberg catalyst) was dissolved in 60 mL of anhydrous THF. The theoretical amount of $LiAlH_4$ necessary to reduce 50% of the ester groups (57 mg, 1.5 mmol) was added in one portion, and the mixture was stirred vigorously at room temperature for 1 h. After the addition of 5 mL of ethyl acetate and stirring for 15 min, 100 mL of a 10% aqueous H_2SO_4 solution was slowly added. The two phases were separated, and the aqueous layer extracted with ethyl acetate. The combined organic phases were washed with H_2O, saturated $NaHCO_3$ solution, brine, and dried over anhydrous magnesium sulfate. After removing the solvent on the rotary evaporator, the resulting white polymer (1.76 g) was dried at 50 ºC under vacuum for 24 h. The same procedure was used to reduce 1.88 g (6.0 mmol) of the PEMO obtained with Vandenberg catalyst in presence of THF. Yield 1.82 g (98%).

^{1}H-NMR ($CDCl_3$, TMS, δ in ppm): 3.63 (s, -O-CH_3), 3.65– 3.55 (t, -CH_2OH), 3.40–3.10 (m, polyether backbone), 2.27 (t, -CH_2-CO_2Me), 1.70–1.10 (m, -CH_2-aliphatic backbone), 0.85 (t, -CH_3).

^{13}C-NMR ($CDCl_3$, TMS, δ in ppm): 174.3 (-CO_2Me), 82–74 (polyether backbone), 62.9 (-CH_2OH), 51.6 (-OMe), 34.2 (-CH_2-CO_2Me), 32.9 (-CH_2-CH_2OH), 32.1 (-CH_2-CH_2-CH_3), 31–25.5 (m, aliphatic backbone), 25.2 (-CH_2-CH_2-CO_2Me), 22.9 (-CH_2-CH_3), 14.3 (-CH_3).

Characterization

GC-MS analyses were done in a 6890N gas chromatograph and a 5973 mass spectrometer (Agilent Technologies, Palo Alto, CA), using a HP-5MS capillary column of 5% phenyl polydimethyl siloxane (30 m, 0.25 mm, and 0.25 μm), from Agilent Technologies, and 99.999% pure helium gas as the carrier at a flow rate of 1.5 mL min^{-1}. Samples were injected in a split/splitless injector at a split ratio of 20:1, at a temperature of 280 ºC. The oven temperature of GC was initially held at 60 ºC, raised to 260 ºC at a rate of 6 ºC min^{-1}, and then held for 50 min. The mass spectrometer acquired data in scan mode with an m/z interval from 35 to 800. The compounds were identified by comparison with NIST08 MS library.

^{1}H-NMR (400 MHz) and ^{13}C-NMR (100.6 MHz) spectra were recorded in $CDCl_3$ and toluene-d_8 using a Varian Gemini 400 spectrometer. Chemical shifts were reported in ppm relative to TMS and $CHCl_3$ as internal standards.

Matrix-assisted laser desorption/ionization Time-of-flight mass spectrometry (MALDI-TOF MS) measurements were performed with a Voyager DE-RP mass spectrometer (Applied Biosystems, Framingham, MA) equipped with a nitrogen laser delivering 3 ns laser pulses at 337 nm. 1,8,9Antracenetriol was used as matrix and potassium trifluoroacetate as dopant. Samples were prepared from a THF solution containing 40 mg/mL of matrix, 3 mg/mL of polymer, and 0.1 mg/mL of dopant. The homogenized mixture was casted in the MALDI plate.

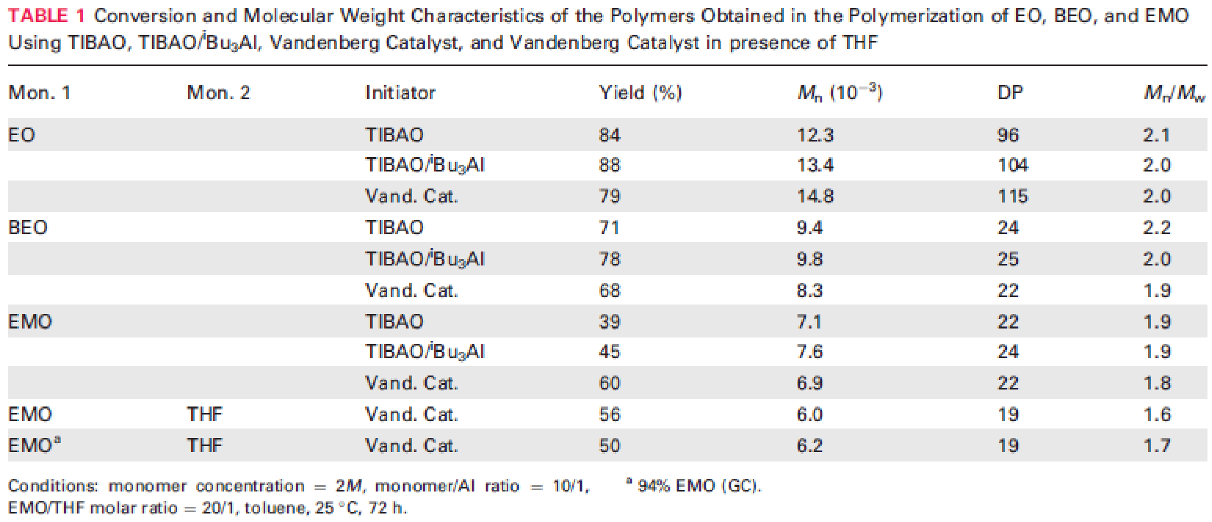

TABLE 1 Conversion and Molecular Weight Characteristics of the Polymers Obtained in the Polymerization of EO, BEO, and EMO Using TIBAO, TIBAO/^{i}Bu$_3$Al, Vandenberg Catalyst, and Vandenberg Catalyst in presence of THF

Mon. 1	Mon. 2	Initiator	Yield (%)	M_n (10^{-3})	DP	M_n/M_w
EO		TIBAO	84	12.3	96	2.1
		TIBAO/^{i}Bu$_3$Al	88	13.4	104	2.0
		Vand. Cat.	79	14.8	115	2.0
BEO		TIBAO	71	9.4	24	2.2
		TIBAO/^{i}Bu$_3$Al	78	9.8	25	2.0
		Vand. Cat.	68	8.3	22	1.9
EMO		TIBAO	39	7.1	22	1.9
		TIBAO/^{i}Bu$_3$Al	45	7.6	24	1.9
		Vand. Cat.	60	6.9	22	1.8
EMO	THF	Vand. Cat.	56	6.0	19	1.6
EMO[a]	THF	Vand. Cat.	50	6.2	19	1.7

Conditions: monomer concentration = 2*M*, monomer/Al ratio = 10/1, EMO/THF molar ratio = 20/1, toluene, 25 °C, 72 h.

[a] 94% EMO (GC).

Size exclusion chromatography (SEC) analysis was carried out with an Agilent 1200 series system with PLgel 3 µm MIXED-E, PLgel 5 µm MIXED-D, and PLgel 20 µm MIXED-A columns in series, and equipped with an Agilent 1100 series refractive-index detector. Calibration curves were based in polystyrene standards having low polydispersities. THF was used as the eluent at a flow rate of 1.0 mL/min, the sample concentrations were 5–10 mg/mL, and injection volumes of 100 µL were used.

RESULTS AND DISCUSSION

The main purpose of this work was the study of the ioniccoordinative polymerization of EMO. In general, internal epoxies are difficult to polymerize because of the low reactivity regarding their high steric hindrance. In addition, the presence of other oxygenated functional groups in the monomer is known to passivate the catalyst active sites and favors the occurrence of side reactions that decreases the yield and molecular weight of the resulting polymers.[26,27,38–40] To further study these effects, we choose three monomers with similar steric hindrance but different coordinative ability: EO, BEO, and EMO (Scheme 1). Only monomers with cis configuration were considered because this is the dominant configuration in natural fatty acids.

Synthesis of EO was accomplished by the Prileshajev epoxidation of pure cis-4-octene with MCPBA following a modified procedure[35] and purified by fractional distillation over CaH_2. For the synthesis of BEO and EMO, benzyl-9-octadecenylether prepared from 85% oleoyl alcohol and two different methyl oleate samples with 90 and 99% of oleic acid methyl ester content were used. The peroxotungstate-catalyzed epoxidation with H_2O_2[34] resulted in excellent yields of EMO and BEO with high purity. The epoxides were purified by a combination of low-temperature crystallization and column chromatography and dried over activated 4 Å molecular sieves. The purity of the monomers was determined by CG-MS and was found over 98% in the case of EO and the EMO obtained from the 99% methyl oleate. The purity of BEO was 94%, with the major impurities being the benzyl ethers of palmitoyl and stearoyl alcohols. In the case of the EMO obtained from the 90% methyl oleate, purity was 96%, with the major impurities being the methyl esters of palmitic, stearic, eicosanoic, docosanoic, and tetracosanoic acids. Pure EMO sample was used to perform the polymerization studies, whereas the EMO obtained from the less-expensive methyl oleate 90plus$^{\text{VR}}$ was used for large-scale polymerizations.

Alkyl- and alkoxyaluminoxane-based catalysts such as Vandenberg catalyst, methylaluminoxane MAO, or TIBAO have been described to be effective in the polymerization of longchain terminal epoxies derived from plant oils.[32,41] With these catalysts, polyethers with molecular weights up to 20 10^5 have been described. Neat aluminum alkyls are known to not initiate the polymerization of epoxides. However, associated with aluminoxanes, effective initiators in the polymerization of epoxides and other compounds are produced.[42] The Vandenberg chelate catalyst ($Et_3Al/AcAc/H_2O$ 1:1:0.5) has also been reported to be effective in the polymerization of methyl 10,11-epoxyundecanoate and other epoxides,[43] but preliminary studies with the methyl 9,10-epoxyoctadecanoate led to very low polymer conversions. So, we selected TIBAO, TIBAO/^{i}Bu$_3$Al (1:1), and the Vandenberg catalyst (Et_3Al/H_2O 1:0.5) as ionic-coordinative catalysts for the polymerization studies.

Catalysts were added at 0 ^{o}C to the monomer dissolved in toluene, and the polymerizations were carried out at 25 C for 3 days to obtain a high monomer conversion. Preliminary studies showed that longer polymerization times did not improve polymer conversion. In all cases, the analyses of the crude polymerization mixtures indicate the presence of considerable amounts of monomer together with low-molecularweight oligomers. This seems to indicate that, after a certain polymerization time, the active sites in the catalyst become no longer active. Polymers were precipitated in methanol containing 5% HCl to solubilize aluminum species and were purified by precipitating twice a THF solution in an excess of methanol. This treatment efficiently removes the oligomeric fraction with no significant reduction in the yield. Typically, for the polymerization of EMO with the Vandenberg catalyst, after polymer work up and two precipitations in methanol, the yield was reduced from 67% to 56%. The soluble fraction was found to be mainly unreacted monomer. In Figure 1, the SEC traces of the PEMO fractionation process are shown. Similar behavior was observed for the rest of polymerizations. Polymer conversion and molecular weight of the different polymers are collected in Table 1. In general, PEO conversions are higher than PBEO and PEMO, and PEMO gives the lowest conversion for all the tested catalysts. A similar trend can be observed from the molecular weight values, which are noticeably higher for PEO than for PEMO. This is in accordance with the increasing basic character of the functional groups present in the molecule, which compete with the oxirane oxygen in the polymerization process. For PEO and PBEO, polydispersities are close to 2 as expected for a cationic coordinative polymerization process. Values slightly lower were obtained for the PEMO prepared with all tested catalysts. This is probably a consequence of the fractionation process, which is more effective for this polymer because of its lower molecular weigh and the higher solubility in methanol of the low-molecular-weight oligomers because of the presence of the ester groups. The structure, composition, and characteristics of polymers were analyzed by NMR spectroscopy and MALDI-TOF-MS spectrometry.

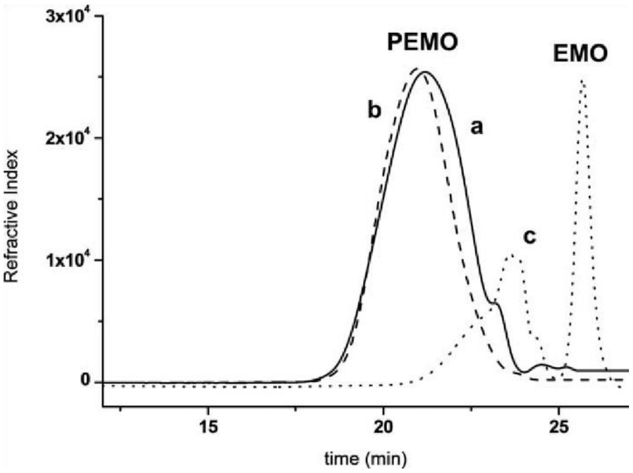

FIGURE 1 SEC traces of the fractions obtained from the crude PEMO prepared with Vandenberg catalyst. (a) PEMO after one precipitation in methanol (continuous line), (b) methanol fraction (dots line), and (c) PEMO after three precipitations in methanol (dashed line).

According to the selected catalyst nature, an ionic-coordinative ring-opening polymerization mechanism is expected for these monomers. Alkylaluminoxanes like MAO have been widely used in the polymerization of olefins, but the polymerization of oxiranes with these catalysts has received much less attention.[32,42] Commercial solutions of aluminoxanes and the Vandenberg catalyst are prepared by reaction of water with a controlled excess of organoaluminum compounds.[31,44] Thus, according to the reaction stoichiometry TIBAO and Vandenberg catalyst are commonly formulated respectively, as $(^{i}Bu)_2Al\text{-}O\text{-}Al(^{i}Bu)_2$ and $(Et)_2Al\text{-}O\text{-}Al(Et)_2$. However, the actual structure is much more complicated and not yet elucidated.[31,45] Both catalysts consist of oligomeric products in which several complex structures coexist in addition to the original component as free and bound species. This means that aluminum and oxygen atoms having different coordinative ability and nucleophilicity coexist in the catalysts.[45] The structure expected from a pure ionic-coordinative polymerization mechanism is a linear polyether ended by a nucleophilic group from the catalyst and one hydroxyl group resulting from the hydrolysis of growing aluminoxane chain end [Scheme 2(a)]. According to the catalyst composition, the group that initiates the polymerization by nucleophilic attack on the oxirane ring should be an alkyl group (ethyl or isobutyl), but it must be considered that hydrolysis of the aluminum alkyls can also produce alkoxy groups.

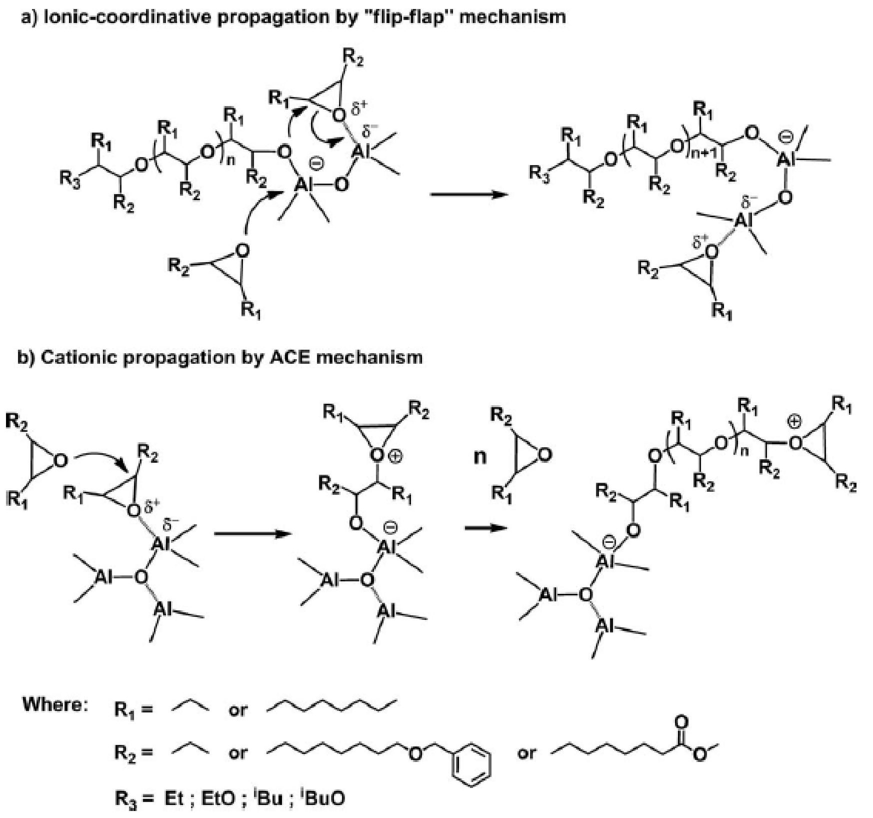

SCHEME 2 Ionic-coordinative and cationic propagation mechanisms.

Ionic-coordinative polymerizations are frequently accompanied by variable amounts of linear and cyclic oligomeric fractions produced by conventional cationic polymerization[38–40] [Scheme 2(b)]. The coexistence of these two polymerization mechanisms must be considered in this case as propagation through an ionic-coordinative mechanism involving a growing chain and a monomer, respectively, bonded and coordinated to two neighboring aluminum atoms. Thus, in the case of internal epoxies bearing long aliphatic chains, the steric requirements would difficult this mechanism favoring the competence of the cationic processes. The end groups expected for lineal polyethers produced by an ACE cationic polymerization mechanism[46] are hydroxy, methoxy, or vinylether units (Scheme 3).

MALDI-TOF-MS analysis of all samples showed a monomodal distribution with lower molecular weight than that obtained by SEC using PS standards. In all cases, several peak populations following a similar pattern can be detected up to masses of 5000–6000 Da. Moreover, in all cases, the maximum peak intensity is centered at around 2000 Da. Taking into account the different molecular weight of the samples analyzed and the similarity between the obtained distributions, it can be inferred that a preferential ionization/volatilization of the fractions of low molecular weight occurs.

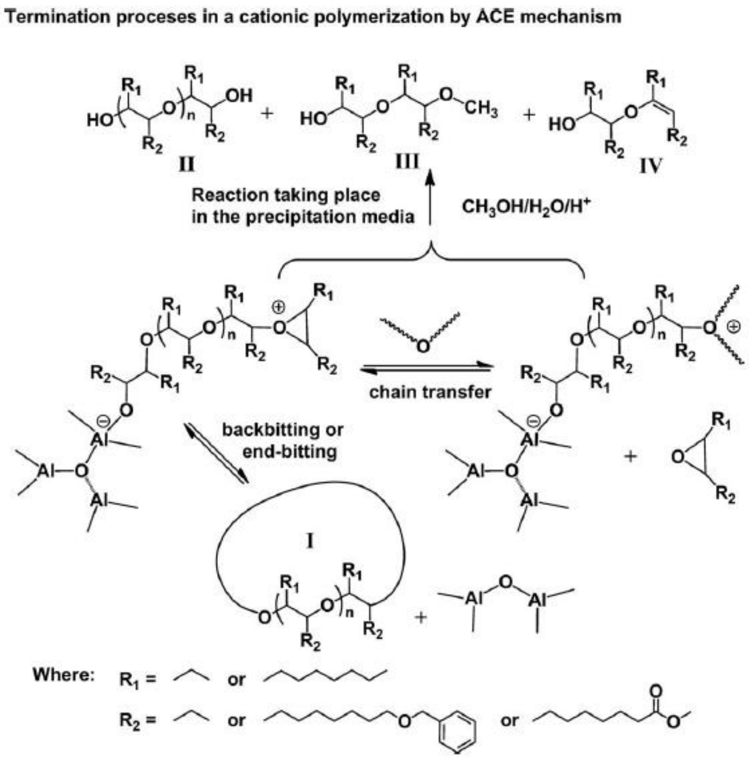

SCHEME 3 Cationic termination mechanism.

The MALDI population pattern changes significantly from one catalyst to another but are very close for PEO and PBEO samples obtained with a same catalyst. In the case of PEMO, some additional peaks are detected, which are related to the presence of a methyl ester group (vide infra). In Figure 2, the MALDI-TOF-MS spectra of PEMO obtained with the different catalysts are shown.

In the case of PEMO obtained with TIBAO [Fig. 2(a)], a cluster of at least 12 different species is observed for each polymerization degree. Peak 2 (nx312.26+K$^+$) can be assigned to both cyclic polyether structures (Species I in Scheme 3) and linear chains terminated by C=C and OH (Species IV in Scheme 3). The intensity of this peak is maximum for n = 5 and decreases rapidly for higher molecular weights. The existence of these cyclic and vinylic structures is relevant as indicated by the competence of the cationic polymerization by ACE mechanism [Scheme 2(b)]. Peak 3 (nx312.26+H_2O+K$^+$), which is the most intense over n = 5, corresponds to linear polyetherdiol structures. Because polymerizations are carried out in absence of water, the two hydroxyl groups must be formed in a final hydrolysis step. Cationic polymerization of EMO with $HSbF_6$ in presence and in absence of water has been reported by us to yield mixtures of cyclic structures and oligoetherdiols;[22] thus, it cannot be excluded that some of these hydroxyl ended polyethers were formed following a cationic mechanism: water and methanol used to stop the polymerization can perform a nucleophilic attack over the different equilibrium tertiary oxonium species[21] (Scheme 3).

Florjanczyk et al.[42] described an alternative ionic-coordinative-based mechanism for the formation of polyetherdiols in the polymerization of PO with MAO and MAO/$AlMe_3$ mixtures. In an ionic-coordinative mechanism, the initiation proceeds by the attack of a nucleophilic group of the catalyst over the oxirane ring coordinated to a neighboring metal center. In the case of aluminoxane-based catalysts, it can be an alkyl or alkoxy group in the aluminum [Scheme 4(a)] or a whole aluminoxane moiety [Scheme 4(b)]. In this last case, the reaction depends on the nucleophilicity of the oxygen in the AlAOAAl bond system. If this oxygen is coordinated to a third aluminum atom [Scheme 2(b)], its nucleophilicity is poor, and a cationic propagation is more likely. If it is not coordinated, their nucleophilicity is higher than the alkyl groups bonded to the aluminum. The polarizability, coordination ability, and polymerization activity of Al-O-Al bonds in this kind of catalysts has been well established.[43,47,48] According to this mechanism [Scheme 4(b)], initiation leads to linear polyethers with Al-O-C bonds at both ends, and their acidic hydrolysis will produce a polyetherdiol. A detailed analysis of the MALDI-TOF spectra allows confirming these hypotheses. Peaks 6 (nx312.26+^{i}Bu+K$^+$) and 7 (nx312.26+^{i}BuO+K$^+$) confirm the attack of the alkyl and alkoxy groups in the Al following an ionic-coordinative mechanism, but their relative low intensity indicates that the predominant nucleophilic attack is produced by aluminoxane groups. Peak 4 (nx312.26+CH_3OH+K$^+$) could be also indicative of the predominance of the ionic-coordinative propagation. Linear polyethers ended by hydroxyl and methoxy groups can be formed by reaction of the oxonium species in the cationic polymerization with the methanolic precipitation media (Species III in Scheme 3). The low intensity of these peaks suggests that cationic processes lead mainly to cyclic structures.[49] Moreover, because water is in low concentration in the precipitation media, the amount of polyetherdiols formed following a cationic process (Species II in Scheme 3) must be low.

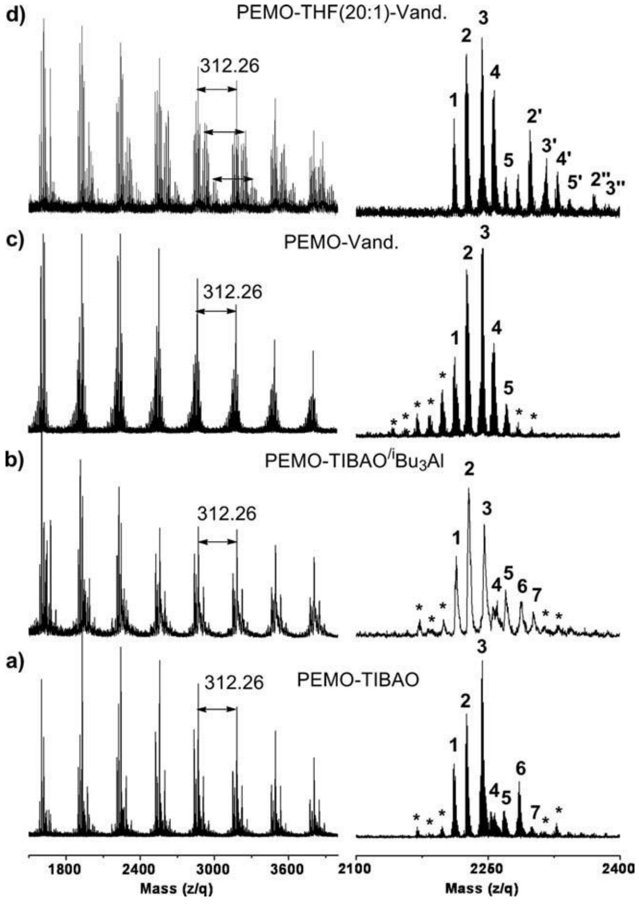

FIGURE 2 Left side: representative fragments of MALDI-TOFMS spectra of the PEMO obtained with (a) TIBAO; (b) TIBAO/ $^{i}Bu_3Al$; (c) Vandenberg catalyst; and (d) PEMO/THF (20:1) with Vandenberg catalyst. Right side: enlargement of the peak corresponding to DP = 7.

Peak 5 ($nx312.26+CH_3OCH_3+K^+$) can be related with linear polyether chains with methoxy groups at both ends. These peaks have low intensity in all the analyzed MALDI-TOF spectrograms and could be origined by acidic methanolysis of the chains ended by aluminum alkoxides at both ends.

The intense Peak 1 and the small peaks marked with asterisks are only observed in PEMO and form a series with $nx312.26-mx15+K^+$ mass units. These peaks are detected in PEMO samples obtained either from 90% or 99% methyl oleate precluding the possibility of the presence of palmitoleic or other C16-C14 acid isomers. Taking into account the presence of methylester groups in the lateral chains, these peaks are likely formed by interaction between the growing chain end and an ester group through a transesterification reaction with the loss of a methyl group for every transesterification process (Scheme 5). This reaction can be intra or intermolecular and supposes, in fact, the termination of the growing chain. Intra- and intermolecular transesterification processes have been fully characterized in the polymerization of lactones.[50,51] The existence of intermolecular transesterification processes is undesirable when the ultimate purpose of these polyethers is the preparation of polyols. As shown in Scheme 5, the polymer resulting from intermolecular transesterification processes contains not only ether linkages but also ester linkages in the polymer main chain; thus, the controlled reduction of side chain ester groups would unavoidably lead to the reduction of the main chain ester groups resulting in a marked decrease in the molecular weight. In the MALDI-TOF of PEMO obtained with TIBAO, the intensity of Peak 1, which corresponds to a single transesterification process, is much higher than peaks marked with asterisk. This seems to indicate that some transesterification reactions are favored, likely the intramolecular between the growing chain end and its own side chain methyl ester due to its favorable entropy. Existence of transesterification reactions also implies that nucleophilic methoxy groups are formed in the media, and, thus, it is likely that some of the polymer chains containing methoxy groups (Peaks 4 and 5) could be also the result of the initiation by these species.

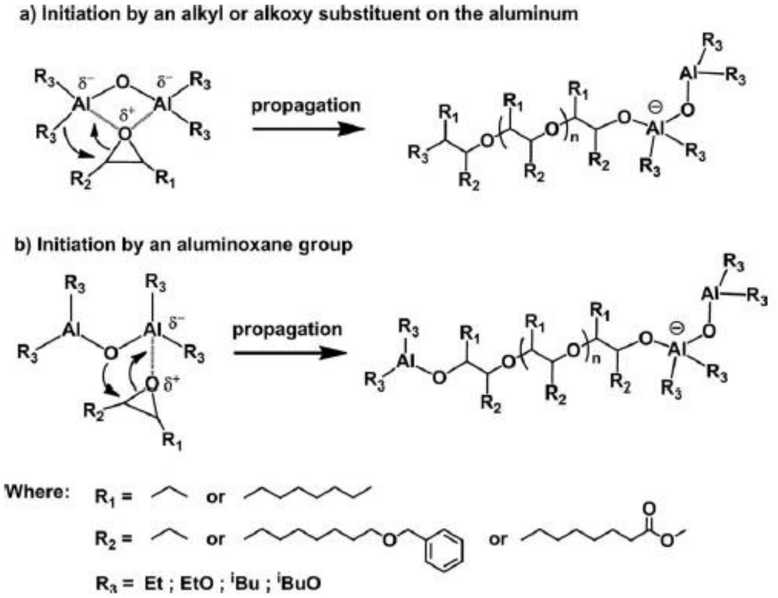

SCHEME 4 Ionic-coordinative initiation mechanism.

It must be pointed out that, in the MALDI-TOF-MS of a sample obtained after 5 h of polymerization (12% polymer conversion), only Peaks 1, 2, 3, and with smaller intensity 6, are detected, suggesting that intermolecular transesterification processes are mainly produced in advanced polymerization stages in which, even if large amounts of monomer remain in the polymerization media, the active sites in the catalyst become no longer active for the coordinative polymerization.

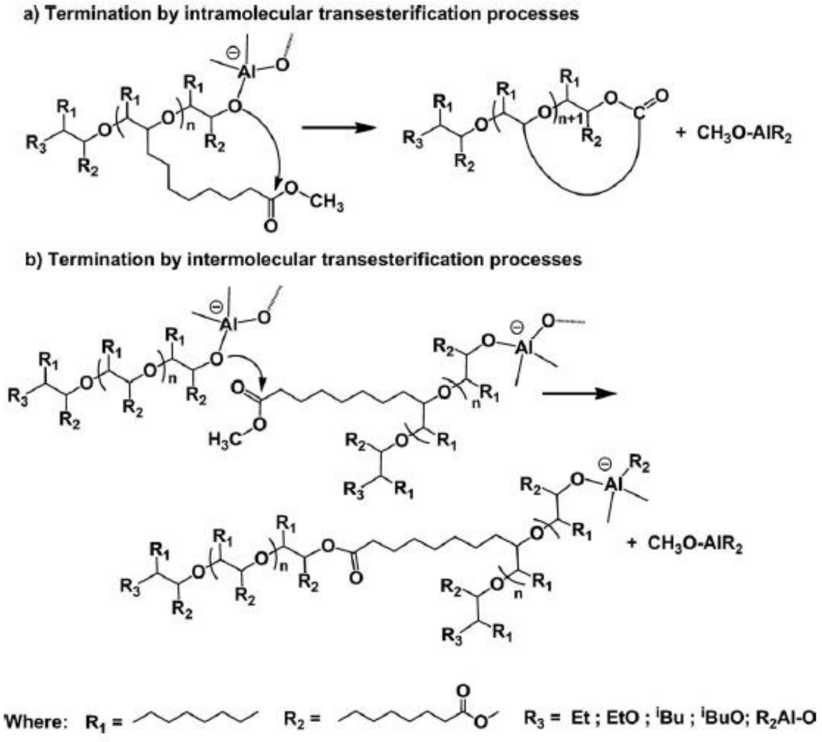

SCHEME 5 Termination by transesterification mechanisms.

In the case of PEMO obtained with the TIBAO/$^{i}Bu_3Al$ system, the MALDI-TOF spectra show the same peak populations with a similar pattern [Fig. 2(b)]. In aluminoxane/trialkylaluminum systems, it has been described that alkylaluminum coordinates to Al-O-Al centers weakening the nucleophilic character of the initiator favoring the attack of monomers over and activated oxirane molecule in a cationic propagation.[42,47,48] PEO, PBEO, and PEMO prepared with this initiator system were obtained in slightly higher yields and molecular weights that those prepared with TIBAO (Table 1). MALDI-TOF analysis reveals that the predominant species, along all the molecular weight range, are cyclic structures [Peak 2 in Fig. 2(b)] as expected for a higher competence of the cationic mechanism because of the presence of $^{i}Bu_3Al$.

MALDI-TOF of PEMO obtained with Vandenberg catalyst show similar species but with a different relative intensity [Fig. 2(c)]. Cyclic structures (Peak 2) and polyetherdiols chains (Peak 3) are detected along all the molecular weight distribution, but the intensity of Peak 2 strongly decreases with the polymerization degree being polyetherdiols the predominant species in the high molecular weight region (PD ≥ 6). This agrees with the prevalence of the ionic-coordinative mechanism for this catalyst. In the case of R_3Al/H_2O catalysts, the presence of small amounts of Al-OH species has been reported,[48] but taking into account that the hydrolysis is always carried out in presence of an excess of R_3Al and that the catalyst solutions are maturated for several days, it is more likely that Al-OR groups are present in the catalyst and not free hydroxyl groups. Peaks corresponding to polymer chains initiated by ethyl groups ($nx312.26+CH_3CH_3+K^+$), which is overlapped with Peak 4 or ethoxy groups (Peak 5, $nx312.26+CH_3CH_2OH+K^+$) can be also detected with low intensity. The most staggering feature is the intensity of Peak 4 ($nx312.26+CH_3OH+K^+$), which is the predominant species in the low-molecular-weight region (PD ≤ 5). This peak, which corresponds to chains initiated by methoxy groups, indicates that for this catalyst transesterification processes are very favored. In this way, a complete set of peaks corresponding to populations derived from these transesterification processes can be detected. This can be observed in more detail in the enlargement shown in Figure 3 in which main structure assignments are done. The peaks marked with an asterisk form a complex series of structures that can be rationalized taking into account the occurrence of one or more transesterification reactions in combination with all above commented basic structures (cycles and hydroxyl, methoxy, or ethoxy ended chains). Some representative examples of these structures are shown in Scheme 6. The main feature of all these branched structures is the presence of one or more ester linkages in the main chain.

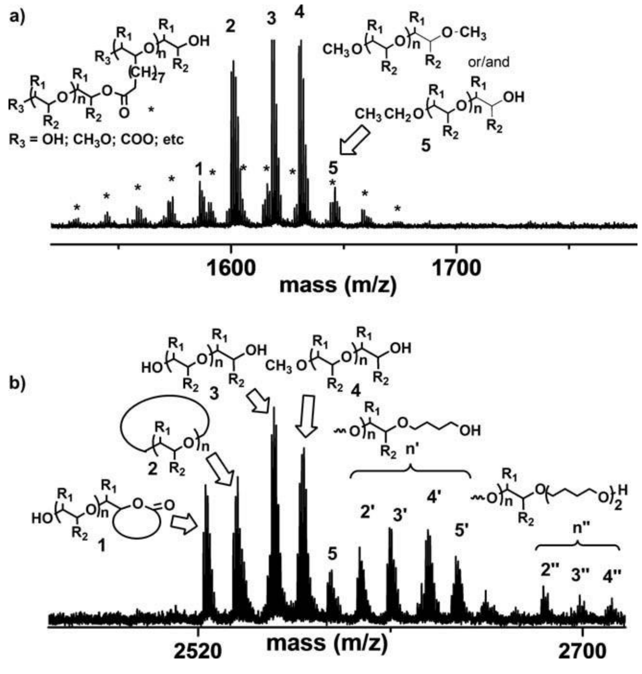

FIGURE 3 Enlarged detail of a peak in the MALDI-TOF-MS spectra of (a) PEMO obtained with Vandenberg catalyst (DP = 5) and (b) PEMO/THF (20:1) with Vandenberg catalyst (DP = 8).

According to Table 1, Vandenberg catalyst affords the best EMO conversion leading to polymers with slightly lower molecular weight than those obtained with TIBAO and TIBAO/^{i}Bu$_3$Al. Thus, Vandenberg catalyst would be the catalyst of choice to obtain PEMO in large scale operations. MALDI analysis indicates that this catalyst produces the highest fraction of polyester type oligomers, which unfortunately would lead to a decrease in the molecular weight by reduction of the ester groups.

As in the case of PEMO obtained with TIBAO, a polymer sample obtained after 5 h of polymerization was analyzed by MALDI-TOF-MS. Again, a simpler pattern composed only by Peaks 1, 2, 3, 4, and 5 (Peaks 1 and 5 with low intensity) was observed. This demonstrates that with the exception of the intramolecular ones, transesterification processes are produced mainly at advanced polymerization stages. Unfortunately, shortening the polymerization time reduces markedly the polymer yield, which, in this case, was only 21% for 5 h.

It has been described that the relative constant rates of the processes involved in a complex polymerization system can be modified by the introduction of a comonomer in the polymerization mixture.[52] The introduction of a monomer with a different reactivity could reduce or suppress some by-side reactions and preferentially activate other propagation steps. In this way, we decided to test the EMO polymerization in presence of a small percentage of other monomer. This comonomer should be able to compete with the methyl ester groups in the reaction with the growing chain ends and must not be reactive enough to compete with EMO in the polymerization. THF was considered a good candidate because it has lower ring strain than oxiranes but higher oxygen basicity.[53] Moreover, THF is known to polymerize and copolymerize with cationic and ionic-coordinative initiators.[54] In this way, its polymerization proceeds at lower rates than epoxies but its coordinative ability is higher and probably enough to compete with the activation of the ester groups by the metallic centers (Scheme 7).

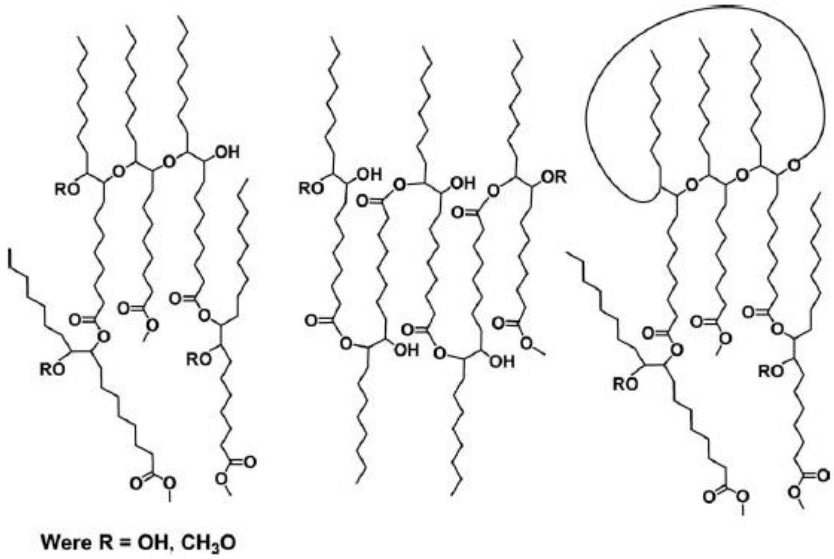

SCHEME 6 Representative polymer structures.

The Vandenberg catalyst copolymerization of EMO with THF in a 20:1 EMO/THF molar ratio was carried out using the same conditions. PEMO-THF was obtained in a slightly lower yield than the homopolymer but with higher yield than the polymerizations with TIBAO and TIBAO/^{i}BuAl$_3$. The SEC analysis shows a small decrease in the molecular weight but a narrower distribution (Table 1).

The MALDI-TOF analysis [Figs. 2(d) and 3(b)] shows some important population differences with PEMO samples obtained in absence of THF. As can be seen, the most intense peaks correspond to the cyclic and the linear polyethers ended by two hydroxyl groups or by one hydroxyl group and a methoxy or ethoxy group. The most relevant feature is the disappearance of the peaks corresponding to multiple transesterification processes with the exception of Peak 1 (nx312.26-15+K$^+$), which has more or less the same relative intensity in the whole range of molecular weights. This peak will be demonstrated (vide infra) to correspond to the intramolecular transesterification processes [Scheme 5(a)]. Moreover, in the MALDI-TOF spectrogram, clusters of the same peak populations at +72 and +2 x 72 mass units can be detected [Fig. 3(b)]. These populations of peaks result from the incorporation of THF units at the different chains. The fact that the incorporation of THF units is only important in the high-molecular-weight region indicates that its copolymerization is produced by the ionic-coordinative mechanism as depicted in Scheme 7. Thus, it can be concluded that the addition of THF as comonomer effectively suppresses the intermolecular transesterification reactions by reacting with the growing chain ends without an important decrease in the molecular weight or the polymer conversion.

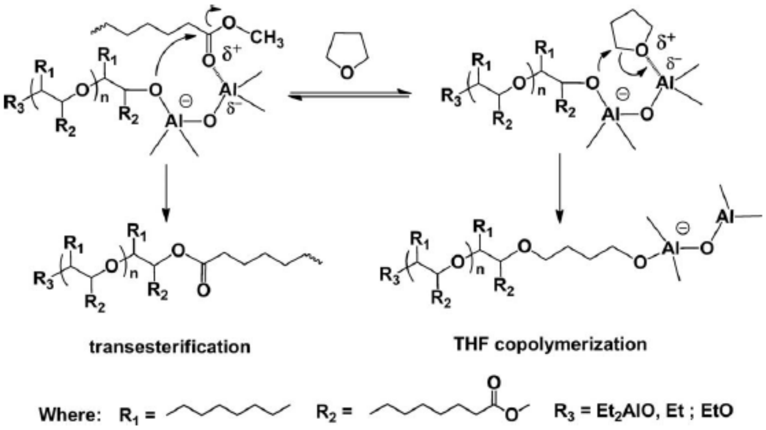

SCHEME 7 EMO polymerization in presence of THF.

To gain more insight about the polymer structure, a reduction experiment was carried out with PEMO samples obtained with Vandenberg catalyst with and without THF. The theoretical amount of $LiAlH_4$ was adjusted to reduce 50% of the ester groups. As can be seen in Figure 4, the SEC traces of the reduced PEMO (1-r) is broader than the starting PEMO (1) and shows a significant decrease in the molecular weight as a consequence of the reduction of the main chain ester groups formed in the transesterification. In the case of PEMO-THF, similar SEC were observed for starting (2) and the reduced product (2-r). This is consistent with the assumption that structures represented by Peak 1 in the MALDI-TOF are cyclic esters resulting from an intramolecular transesterification process, so their reduction do not affect the molecular weight.

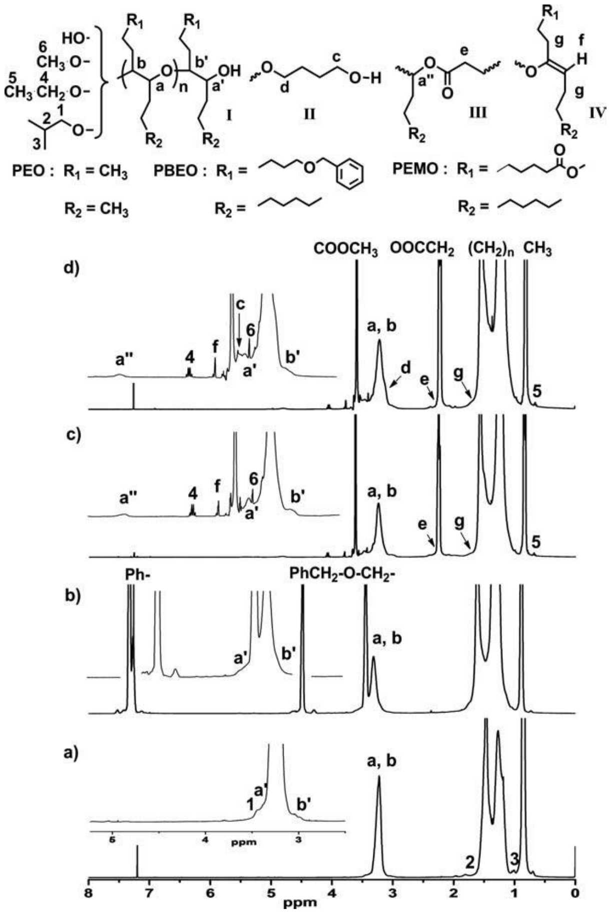

FIGURE 5 ^{1}H-NMR spectra of (a) PEO obtained with TIBAO; (b) PBEO obtained with TIBAO/^{i}Bu$_3$Al; (c) PEMO obtained with Vandenberg catalyst; and (d) PEMO-THF (20:1) obtained with Vandenberg catalyst.

The obtained polymers were also characterized by ^{1}H- and ^{13}C-NMR spectroscopy. Moreover, to confirm the assignments, gHSQC correlation experiments and derivatizations with trichloroacetylisocyanate (TAI) were carried out. Figure 5 shows some representative ^{1}H-NMR spectra with the assignments. The most outstanding feature in all these spectra is that the main chain methyne protons a and b (3.1–3.3 ppm) appear as a narrow signal, whereas in the case of PEMO obtained by cationic polymerization, a broad irregular signal is observed.[22] This indicates certain degree of chain regularity, which further supports the predominance of the ionic coordinative mechanism. Spectrum (a) in Figure 5 corresponds to PEO obtained with TIBAO. Because of its high molecular weight, signals corresponding to end groups have very low intensity.

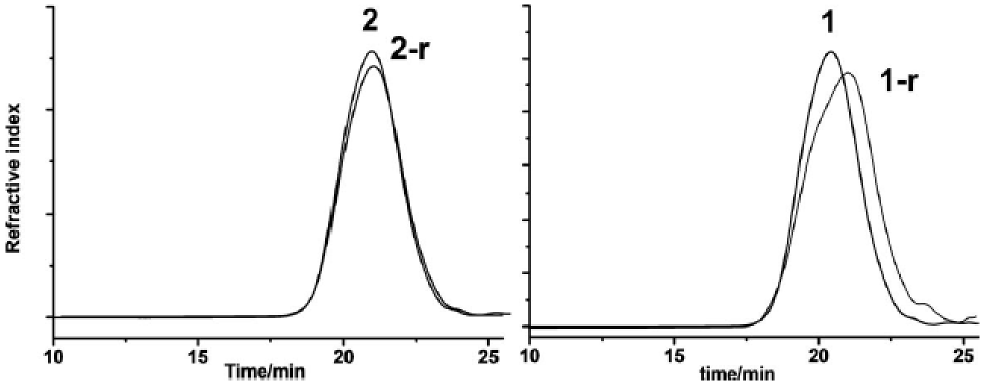

FIGURE 4 SEC traces of PEMO (**1**) and its reduction product (**1-r**), and PEMO-THF (**2**) and its reduction product (**2-r**).

Despite this, broad signals at approximately 3.05 and 3.45 ppm can be detected as shoulders in the methine main chain peak. These signals are observed in all the polymers obtained with the different catalysts and are shifted when the polymer is derivatized with TAI. Thus, they can be assigned to the methine protons of the hydroxylic chain end (a′ and b′ in structure I).

Moreover, in this spectrum, small signals attributable to the protons of isobutoxy end groups (1, 2, and 3 in structure I) can be also detected. In spectrum (b), corresponding to PBEO obtained with TIBAO/^{i}Bu$_3$Al apart from the signals at 3.44 and 4.48 ppm corresponding to the Ph-CH$_2$-O-CH$_2$- side chain groups, the same end group signals can be observed but with lower intensity as expected because of its higher content of cyclic structures. Spectra (c) and (d) correspond, respectively, to PEMO and PEMO-THF (20:1) samples obtained with Vandenberg catalyst. The signals of the methylene and methyl in the -CH$_2$-COOCH$_3$ side chain groups appear, respectively, at 2.28 and 3.68 ppm. In this case, end-group signals can be detected with some intensity because of the lower molecular weight of these polymers. Both spectra are very similar, but in the case of PEMO-THF, two new broad signals at 3.55 and 3.20 ppm are observed, which can be assigned to methylenes c and d in the THF moieties (structure II). Signal c is also shifted downfield when the polymer is derivatized with TAI, and, thus, it can be assigned to the final CH$_2$OH groups. Moreover, in both spectra, small signals at 4.80, 4.05, and 3.77 ppm can be detected. Signal at 4.80 ppm can be assigned to the methine units bonded to an ester group (a″ in structure III). Because this signal appears in both polymers, it must correspond to the intramolecular transesterified species, which are the only ones in PEMO-THF and the predominant in PEMO. Methylene signals of transesterified moieties e overlap with the intense signal of the methylene -CH$_2$-COOCH$_3$ peak.

The quadruplet at 4.05 ppm corresponds to a methylene related to the methyl signal at 0.66 ppm (signal 5), which can be assigned to an ethoxy group. In the case of Vandenberg catalyst, the initiation by ethoxy groups formed during the Et$_3$Al-controlled hydrolysis is one of the more likely coordinative mechanisms. These species (Peak 5 in Figs. 2 and 3) have low relative abundance in the low-molecularweight region of the MALDI-TOF-MS spectra, but they become more and more important as the polymerization degree increases. Moreover, it must be pointed out that ethoxy-initiated species constitutes prominent peaks in the MALDI-TOF-MS spectra of PEO and PBEO obtained with the same catalyst.

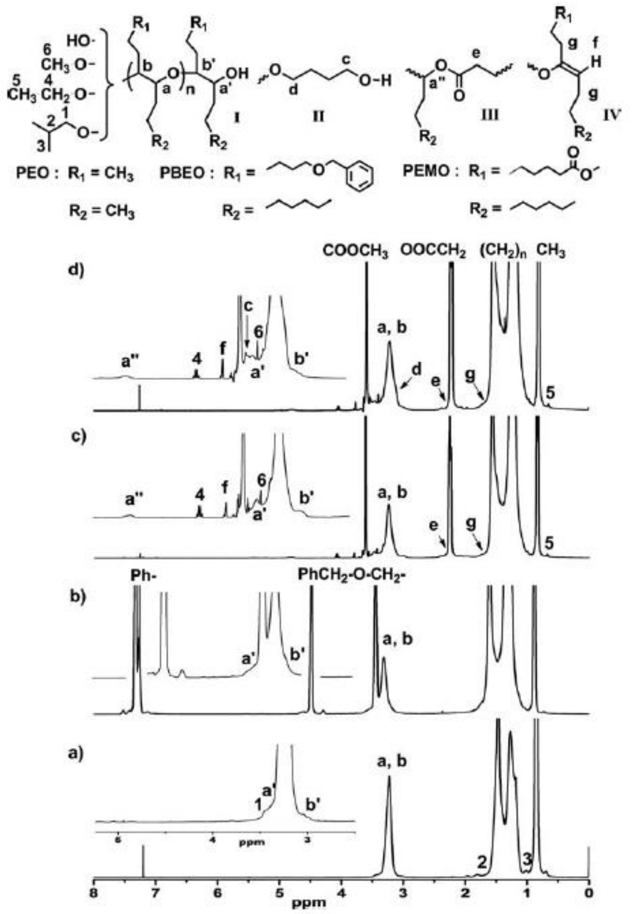

FIGURE 5 ^{1}H-NMR spectra of (a) PEO obtained with TIBAO; (b) PBEO obtained with TIBAO/^{i}Bu$_3$Al; (c) PEMO obtained with Vandenberg catalyst; and (d) PEMO-THF (20:1) obtained with Vandenberg catalyst.

Singlet at 3.77 ppm can be also observed in PEO and PBEO, but its intensity is higher for polymers obtained with Vandenberg catalyst. This signal is related with a methylene that appears as a shoulder at 1.75 ppm. These signals are consistent with a vinylether chain end formed by proton elimination of the growing cationic chain end (structure IV in Scheme 3). This result is very outstanding because until now it was assumed that Peak 2 in the MALDI-TOF-MS spectra corresponds only to cyclic structures. The low intensity of these vinyl signals in the case of polymers obtained with TIBAO and TIBAO/^{i}BuAl$_3$ confirms this assignment. However, for polymers obtained with Vandenberg catalyst, the NMR data seem to indicate that vinylic structures also contribute in some extent. The rest of small signals are not easily identifiable because of its overlapping, and the lack of proper models but the singlet at 3.40 ppm is likely due to the methoxy chain end groups.

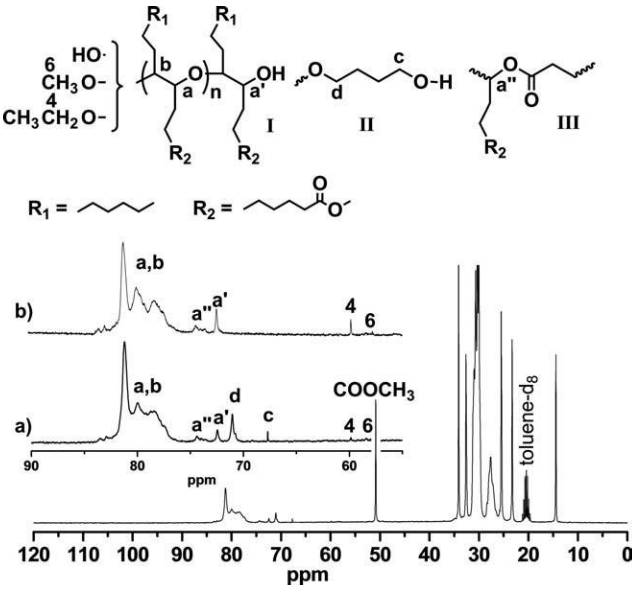

FIGURE 6 ^{13}C-NMR spectra recorded in toluene-d$_8$ of PEMO-THF and its expanded region from 55 to 90 ppm (a) and (b) expanded region for PEMO. Both obtained with Vandenberg catalyst.

Figure 6 shows the ^{13}C-NMR spectrum of PEMO-THF obtained with Vandenberg catalyst and the expanded region between 55 and 90 ppm (a) and the expanded region for PEMO obtained with Vandenberg catalyst (b). Again, the most important feature in all the spectra is the shape of the methine carbons of the repeating unit, which appear as a triad at 80.50, 80.02, and 89.2 ppm with maximum intensity for the former peak. Tacticity has been described for the methyne and methylene carbons of terminal long chain epoxides when polymerized with coordinative initiators,[32] but, in this case, a selective polymerization process is hard to expect owing to the similarity between the two epoxide substituents even the coordination of the ester group in the side chain could favor at least some regioselective polymerization. In the same region of the ^{13}C-NMR spectra, some other smallintensity signals can be observed. The signal at 74.50 ppm, which is a methine, has been assigned to a″ in structure III taking into account its correspondence with the signal at 4.9 ppm in the ^{1}H-NMR spectrum. The signal at 71.0 ppm, which appears in both polymers, corresponds to the methine a′ in the hydroxylic chain ends. The small signals at 59.98 and 58.20 ppm can be assigned, respectively, to the ethoxy and methoxy end groups. Moreover, in the spectra of PEMO-THF, two additional peaks can be observed, which are related with the additional peaks at 3.55 and 3.20 ppm in the ^{1}H-NMR spectrum. These signals correspond to the methylenes c and d (structure II) of the THF moieties. The higher intensity of d indicates that not all THF units are end groups.

Finally, even no specific study was made to optimize polymerization conditions, we assayed the polymerization of EMO with the Vandenberg catalyst in presence of THF in a larger scale (0.1 mol). In this case, we used EMO obtained from 90% methyl oleate, which is 94% pure according to GC analysis and the same polymerization conditions. As can be seen in Table 1, the polymer conversion was slightly lower, but the polymer characteristics are very similar proving that this polymerization procedure can be used to produce comb-like polyethers in acceptable good yields. The synthesis of polyether polyols containing different hydroxyl content from PEMO and its use in the preparation of conventional and segmented polyurethanes is discussed in a next article.[55]

CONCLUSIONS

The coordinative polymerization of methyl epoxyoleate, a derivative from high oleic sunflower oil, and some structural analogues has been investigated. Under mild conditions, ionic-coordinative initiators yield polymers with higher molecular weight than that obtained with conventional cationic catalysts. MALDI-TOF-MS analysis and ^{1}H- and ^{13}C-NMR characterization reveals that obtained polymers consist of a mixture of cyclic and linear structures with different end groups depending on the initiator used. This can be rationalized by the coexistence of ionic-coordinative, which is predominant, and cationic propagation mechanisms. The initiator activity, from polymer conversion, increases from TIBAO to TIBAO/^{i}Bu$_3$Al and to Vandenberg catalyst even a slightly decrease in the polymer molecular weight is produced. At advanced polymerization stages, transesterification processes lead to the formation of branched structures containing ester groups in the main chain. These processes, which limit the use of these polymers in the preparation of renewable polyether polyols, can be suppressed by copolymerizing the methyl epoxyoleate with a small amount of THF. The largescale polymerization of technical-grade methyl epoxyoleate and the reduction of the ester groups of the resulting polyether prove the applicability of this synthetic approach to produce fully renewable predominantly linear polyether polyols of 6000–8000 Da molecular weight with controlled hydroxyl content.

The authors thank MICINN (Comisio´n Interministerial de Ciencia y Tecnologı´a) (MAT2008-01412) for financial support of this work.

REFERENCES AND NOTES

1 Belgacem, M. N.; Gandini, A. Monomers, Polymers and Composites from Renewable Resources; Elsevier: Oxford, 2008.

2 Gu¨ner, F. S.; Yagci, Y.; Erciyes, A. T. Prog Polym Sci 2006, 31, 633–679.

3 Meier, M. A. R.; Metzger, J. O.; Shubert, U. S. Chem Soc Rev 2007, 36, 1788–1802.

4 (a) Sharma, V.; Kundu, P. P. Prog Polym Sci 2008, 33, 1199–1215; (b) Sharma, V.; Kundu, P. P. Prog Polym Sci 2006, 31, 983–1008.

5 Lu, Y.; Larock, R. C. ChemSusChem 2009, 2, 136–147.

6 Biermann, U.; Friedt, W.; Lang, S.; Lu¨hs, W.; Machmu¨ller, G.; Metzger, J. O.; Ru¨sch Gen Klaas, M.; Scha¨fer, H. J.; Schneider, M. P. Angew Chem Int Ed Engl 2000, 39, 2206–2224.

7 Findley, T. W.; Swern, D.; Scalan, J. T. J Am Chem Soc 1945, 67, 412–414.

8 Rangarajan, B.; Havey, A.; Grulke, E. A.; Culnan, P. D. J Am Oil Chem Soc 1995, 72, 1161–1169.

9 Grigoropoulou, G.; Clark, J. H.; Elings J. A. Green Chem 2003, 5, 1–7.

10 Lane, B. S.; Burgess, K. Chem Rev 2003, 103, 2457–2473.

11 Orellana-Coca, C.; Camocho, S.; Adlercreutz, D.; Mattiasson, B.; Hatti-Kaul, R. Eur J Lipid Sci Technol 2005, 107, 864–870.

12 Sobczak, J. M.; Ziolkowski J. J. Appl Cat A: Gen 2003, 248, 261–268.

13 Abdullah, B. M.; Salimon J. J Appl Sci 2010, 10, 1545–1553. 14 Crivello, J. V.; Narayan, R. Chem Mater 1992, 4, 692–699.

15 Guo, A.; Demydov, D.; Zhang, W.; Petrovic, Z. S. J Polym Environ 2002, 10, 49–52.

16 Guo, A.; Javni, I.; Petrovic, Z. J Appl Polym Sci 2000, 77, 467–473.

17 Petrovic, Z.; Guo, A.; Javni, I. U.S. Patent 6,107,433, 2000.

18 Dietrich, D.; Uhlig, K. In Ullmann's Encyclopedia of Industrial Chemistry; Elvers, B.; Hawkins, S.; Schulz, G., Eds.; VCH: Weinheim, 1992; p 665.

19 Chakrapani, S.; Crivello, J. V. J Macromol Sci Pure Appl Chem 1998, 35, 1–20.

20 Crivello, J. V.; Carlson, K. D. J Macromol Sci Pure Appl Chem 1996, 33, 251–262.

21 Warwel, S.; Fehling, E.; Kunz, M. Eur J Lipid Sci Technol 2001, 103, 133–140.

22 Lligadas, G.; Ronda, J. C.; Galia`, M.; Biermann, U.; Metzger, J. O. J Polym Sci Part A: Polym Chem 2005, 44, 634–645.

23 Booth, C.; Higginson, C. E.; Powell, E. Polymer 1964, 5, 479–497. 24 Vandenberg, E. J. J Polym Sci Part A-1 1969, 7, 525–567.

25 Yoshino, N.; Suzuki, C.; Kobayashi, H.; Tsuruta, T. Makromol Chem 1988, 189, 1903–1913.

26 Ronda, J. C.; Serra, A.; Mantecon, A.; Cadiz, V. React Funct Polym 1995, 28, 1–11.

27 Shih, J. S.; Tirrell, D. A. J Polym Sci Polym Chem Ed 1984, 12, 781–791.

28 Vogl, O.; Muggee, J.; Bansleben, D. Polym J 1980, 12, 667–686.

29 Bansleben, D. A.; Vogl, O. J Polym Sci Polym Chem Ed 1985, 23, 673–701.

30 Muggee, J.; Vogl, O. J Polym Sci Polym Chem Ed 1986, 24, 2327–2349.

31 Boleslawski, M.; Serwatowski, J. J Org Chem 1983, 254, 159–166.

32 Warwel, S.; Wiege, B.; Fehling, E.; Kunz, M. Eur Polym J 2000, 36, 2655–2663.

33 Sato, K.; Auki, M.; Ogawa, M.; Hashimoto, T.; Noyori, R. J Org Chem 1996, 61, 8310–8311.

34 Venturello, C.; D'Aloisio, R. J Org Chem 1988, 53, 1553–1557.

35 Kishi, Y.; Aratani, M.; Tanino, H.; Fukuyama, T.; Goto, T. J Chem Soc Chem Commun 1972, 20, 64–65.

36 Mai, E.; Schneider, C. Chem Eur J 2007, 13, 2729–2741.

37 Vogel's Textbook of Quantitative Chemical Analysis, 5th ed.; Jeffery, G. H.; Bassett, J.; Mendham, J.; Denney, R. C., Eds.; John Wiley & Sons: New York, 1989; p 446.

38 Ronda, J. C.; Serra, A.; Cadiz, V. Macromol Chem Phys 1997, 198, 2917–2934.

39 Ronda, J. C.; Serra, A.; Cadiz, V. Macromol Chem Phys 1997, 198, 2935–2948.

40 Ronda, J. C.; Serra, A.; Cadiz, V. Macromol Chem Phys 1999, 200, 221–230.

41 Vogl, O.; Kiliman, L. B. J Macromol Sci Pure Appl Chem 2001, A38, 91–105, 123–135.

42 Florjanczyk, Z.; Plichta, A.; Sobczak, M. Polymer 2006, 47, 1081–1090.

43 Bansleben, D. A.; Hersman, M. J.; Vogl, O. J Polym Sci Polym Chem Ed 1984, 22, 2489–2500.

44 Vandenberg, E. J. J Polym Sci Polym Chem 1985, 23, 915–949.

45 Rytter, E.; Stovneng, J. A.; Eilersen, J. L.; Ystenes, M. Organometallics 2001, 20, 4466–4468.

46 Kubisa, P. Makromol Chem Macromol Symp 1988, 13/14, 203–210.

47 Ueyama, N.; Araki, T.; Tani, H. Inorg Chem 1973, 12, 2218–2225.

48 Ueyama, N.; Araki, T.; Tani, H. Macromolecules 1974, 7, 153–160.

49 Goethals, E. J. Adv Polym Sci 1977, 23, 103–130.

50 Albertsson, A.-C.; Varma, I. K. Biomacromolecules 2003, 4, 1466–1486.

51 Tang, M.; White, A. J. P.; Stevens, M. M.; Williams, C. K. Chem Commun 2009, 941–943.

52 Bednarek, M.; Kubisa, P.; Penczek, S. Macromolecules 1999, 32, 5257–5263.

53 Aoki, S.; Harita, Y.; Tanaka, Y.; Mandai, H.; Otsu, T. J Polym Sci Part A: Polym Chem 1968, 6, 2585–2590.

54 Vandenberg, E. J.; Mullis, J. C. J Polym Sci Part A: Polym Chem 1991, 29, 1421–1438.

55 Del Rio, E.; Lligadas, G.; Ronda, J. C.; Galia, M.; Cadiz, V. J Polym Sci Part A: Polym Chem; Doi: 10.1002/pola.24296.